MIT Open Access Articles

Simplified vehicle–bridge interaction for medium to long-span bridges subject to random traffic load

Massachusetts Institute of Technology

Simplified vehicle–bridge interaction for medium to long-span bridges subject to random traffic load

S   V   -B   I   M
L   -   B   S   R   T   L

A P

Soheil S. Eshkevari[*]
Department of Civil and Environmental Engineering
Lehigh University
Bethlehem, PA 18015
ses516@lehigh.edu

Thomas J. Matarazzo[†]
Senseable City Lab
Massachusetts Institute of Technology
Cambridge, MA 02139
Information Science
Cornell Tech
New York, NY 10044
tomjmat@mit.edu

Shamim N. Pakzad
Department of Civil and Environmental Engineering
Lehigh University
Bethlehem, PA 18015
pakzad@lehigh.edu

May 26, 2020

A

This study introduces a simplified model for bridge-vehicle interaction for medium- to long-span bridges subject to random traffic loads. Previous studies have focused on calculating the exact response of the vehicle or the bridge based on an interaction force derived from the compatibility between two systems. This process requires multiple iterations per time step per vehicle until the compatibility is reached. When a network of vehicles is considered, the compatibility equation turns to a system of coupled equations which dramatically increases the complexity of the convergence process. In this study, we simplify the problem into two sub-problems that are decoupled: (a) a bridge subject to a random excitation, and (b) individual sensing agents that are subject to linear superposition of the bridge response and the road profile roughness. The study provides sufficient evidences to confirm that the simulation approach is valid with minimal error when the bridge span is medium to long, and the spatio-temporal load pattern can be modeled as random white noise. The latter assumption is verified using a comparative study on a random traffic network. Quantitatively, the proposed approach is over 1,000 times more computationally efficient when compared to the conventional approach for a 500 m long bridge, with response prediction errors below 0.1%.

1 Introduction

The problem of vehicle-bridge interaction (VBI) has been studied widely over recent years due to the broad applications spanning from fatigue analysis and bridge mobile sensing [Chen and Cai, 2007, Zhu and Law, 2015, 2016, Yang and Yang, 2018, Sadeghi Eshkevari et al., 2020a] to ride comfort and safety analysis [Zhou and Chen, 2016, Camara et al., 2019]. The complexity of the problem has resulted in a reliance on numerical modeling to evaluate research hypotheses [Yang et al., 2004a, Malekjafarian and OBrien, 2014, Sadeghi Eshkevari et al., 2020b]. Consequently, today various numerical tools for VBI modeling are available, yet the majority are geared towards problems concerning individual

---

[*]ses516@lehigh.edu

[†]tomjmat@mit.edu

vehicle dynamics, e.g., a single vehicle's interaction with a simple bridge. Recent applications on vehicle fleets and crowdsensing methods [O'Keeffe et al., 2019, Matarazzo et al., 2018] have provided insight into the wealth of SHM information that can be produced by ubiquitous mobile sensors. Such large-scale analyses call for interaction methods that can incorporate vehicular networks and everyday traffic scenarios, and are computationally efficient.

1.1 Crowdsensing the Built Environment with Mobile Sensors

The growing adaptation of *internet of things* technologies and connected devices in smart cities suggest a new sensing paradigm in which new information is regularly gathered from the crowd, e.g., individual smartphones, vehicular sensor networks, etc. Calabrese et al. [2010] proposed a real-time data aggregation solution for constructing a dynamic urban map of large cities using crowdsourced smartphone data. Wang et al. [2012] quantified traffic patterns and proposed management applications based on large-scale mobile phone data. Yu et al. [2015] successfully utilized smartphone sensors for structural health monitoring application due to its availability and inexpensive data acquisition. Feng et al. [2015], Ozer et al. [2015] also suggested novel applications in post-event bridge vibration analysis using stationary smartphones as sensors.
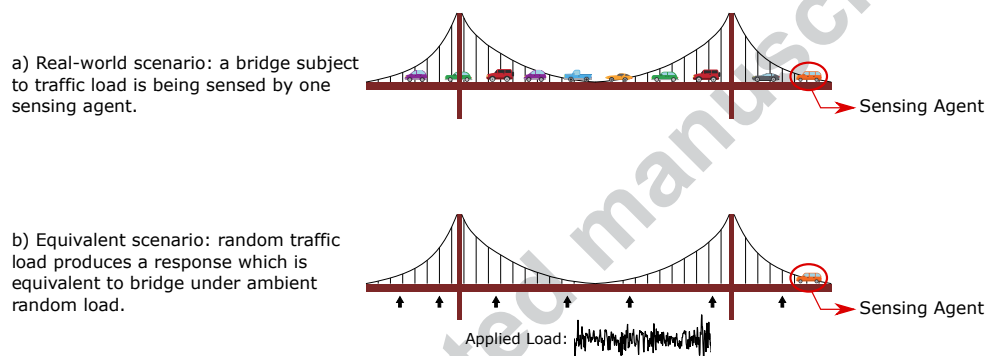

Figure 1: Crowdsourcing framework. The sensing agent is one (or more) particular vehicle within a large pool of crossing vehicles. The problem is equivalent to a case in which the bridge is subject to ambient random load while being scanned by the sensing agent.

Crowdsensing inherently relies on *mobile sensor networks*, which is an emerging data acquisition technique in structural health monitoring (SHM). Historically, observations of structural dynamics have been based on measurements collected by *fixed sensor networks*. Alternatively, Figure 1 illustrates how a vehicle can act as a sensing agent amongst bridge traffic. Matarazzo and Pakzad [2016] presented the STRIDE modal identification algorithm and verified that mobile sensor data was suitable for a comprehensive modal identification (frequencies, damping ratios, and mode shapes). They proposed the truncated physical state-space model as an efficient approach for representing time-space observations from a mobile sensor network. Later, Matarazzo and Pakzad [2018] presented an identification algorithm called STRIDEX to identify truncated physical model parameters, which enabled efficient and scalable modal identification using mobile sensors; the study showed that in an experimental case, one mobile sensor provided a mode shape density comparable to 120 fixed sensors. As a versatile alternative for STRIDEX, Sadeghi Eshkevari et al. [Sadeghi Eshkevari et al., 2020b, Eshkevari and Pakzad, 2020] proposed a method called MIMC to consider vibration data collected by multiple mobile sensors with uncontrolled motions which successfully identified comprehensive bridge modal properties in different simulated applications.

The idea of smartphone data crowdsourcing for bridge system identification has been recently tested on real bridges. Matarazzo et al. [2018] presented a real-world application of mobile sensors, in the form of smartphones in moving vehicles. Significant indicators of the first three modal frequencies of the Harvard Bridge were found by aggregating data from about forty bridge trips. This study shows promising results for the use of crowdsensing in bridge health monitoring. Yet further development is needed, in particular, analytical and experimental studies on mobile sensing using data crowdsourcing, to attain the sophistication and robustness of the traditional modal identification methods based on fixed sensor data.

1.2 Vehicle-Bridge Interaction Modeling

More practical approaches for bridge health monitoring such as crowdsensing require a computationally scalable numerical framework. A comprehensive literature review of common VBI simulation approaches is provided by

González [2010]. Initially, the vehicle-bridge interaction was modeled using 1D continuous beam models subject to simple moving loads [Frỳba, 2013] which is solvable in closed-form. By further development of computers and increasing use of the finite element method, the problem was reframed as a multi degrees of freedom (MDOF) system for the bridge interacting with simplified dynamical models of the vehicle. This approach has been broadly adopted for VBI modeling, mostly for short to mid-span bridges subject to a very limited number of vehicles with controlled motions. In this approach, once the models for the vehicle and the bridge are selected (based on required accuracy and fidelity), the dynamic equations of each component are separately built, in which the interaction forces between the vehicle and the bridge are coupled to the both sets of equations. Therefore, a numerical solver is required to solve the problem either iteratively or as a coupled system of equations.

The underlying principle of the approach, that is the interactive dynamic force acting between the vehicle and the bridge, has remained consistent throughout the literature. The uncoupled iterative algorithm is the most common method for VBI problems [Lin and Yang, 2005, Kim and Kawatani, 2008, OBrien et al., 2010, González et al., 2012, Yang and Yang, 2018]. Various versions of the algorithm have been developed based on the problem requirements, e.g., different vehicle models, single DOF, quarter-car, or half-car models as well as different bridge models with different fidelity levels (such as 2D, 3D, with or without material or geometrical nonlinearities). However, in the majority of these studies, a short- to mid-span bridge has been considered. As mentioned in González [2010], when the vehicle mass is negligible compared to the bridge mass (which is the case for medium to long bridges) and a smooth pavement is assumed, the dynamic model of the vehicle can be replaced with a moving mass model that simplifies the simulation process. Road irregularities increase the contribution of vehicle dynamics to the interaction force, which emphasize on the importance of a fully coupled model.

In the uncoupled iterative approach, the bridge model is analyzed multiple times (once at the beginning, and at least once for each time step inside the compatibility convergence loop). In addition, as the bridge dimension grows, an accurate bridge model requires more degrees of freedom, which increases the computational costs. A limited number of studies have considered long-span bridges along with a dense vehicle network for the simulation purpose. Camara et al. [2019] recently modeled wind-bridge-vehicle interaction using the uncoupled iterative approach. The study could accurately model the system by adopting complex models for each component. The complexity of the approach implies that it requires great efforts to built such a high fidelity model, which may neither be a feasible nor cost effective solution for crowdsensing or other crude vehicle-bridge interacting scenarios. Moreover, bridge standards recommend lower dynamic factors for live loads in medium to long bridges compared to short bridges [AASHTO, 2008]; which means that the VBI interaction force is less dynamic and more similar to a constant moving load. These challenges and specifications suggest that it may not be required to use rigorous iterative solutions for VBI simulation of medium to long bridges subject to high traffic loads. This study intends to demonstrate that a simplified simulation approach inspired by the conventional uncoupled iterative algorithm [González, 2010] is able to simulate VBI problems with high accuracy and dramatically less computational effort.

Figure 1 shows how the same notion is applicable in the VBI simulation. This figure demonstrates a scenario of interest in which the bridge is subject to a random traffic network. The objective is to simulate the system and finally calculate the collected response of the sensing agent. In a brute-force approach, the spatial coordinates and mechanical properties of every single vehicle in the network are required to fully determine the complex model. Such an accurate information setting is quite impractical and unnecessary. Alternatively, one can simulate the collective loading effect of the vehicle network (the sensing agent excluded) by ambient random load (as shown in Figure 1 - b). If the spatio-temporal ambient random load is represented as a matrix F_0, the conventional algorithm for simulating the VBI problem is as shown in Algorithm 1.

In this algorithm, $M_{brg}, C_{brg}, K_{brg}$ and $M_{vcl}, C_{vcl}, K_{vcl}$ characterize mechanical properties of the bridge and the vehicle, respectively. rgh is a vector of roughness profile elevations at bridge DOFs. The algorithm performs the following steps:

1. The bridge is subjected to random ambient load F_0 at different physical locations.

2. A vehicle starts moving from one side of the bridge and at each time instance, the bridge response (displacement) from the previous step in addition to the local roughness intensity (i.e., $rgh(t)$) is input to the vehicle system.

3. The vehicle response to the applied force from the previous step is then analyzed using a Matlab ordinary differential equation (ODE) solver to calculate its displacement response (line 9 in Algorithm 1). Based on this response, the interacting force between the sensing vehicle and the bridge is calculated as: $F_t = -K_{vcl}[2](y_{vcl}(t) - wv) - C_{vcl}[2](y'_{vcl}(t) - wv')$ (where [2] stands for the 2nd DOF of the vehicle, i.e., the tire). Note that if $F_t < 0$, it is replaced with zero since it means that the vehicle lost its contact.

3

Algorithm 1 Conventional iterative VBI simulation.

1: **Input**: $M_{brg}, C_{brg}, K_{brg}, M_{vcl}, C_{vcl}, K_{vcl}, F_0, rgh$
2: $Y_{brg} = Newmark\beta(M_{brg}, C_{brg}, K_{brg}, F_0)$
3: **for** t = 1, $\cdots$, T **do**
4:     Initiate $r := 0, r_n := some\ large\ value$
5:     **while** $abs(r - r_n) < threshold$ **do**
6:         $r = Y_{brg}(t)$
7:         $wv = rgh(t) + r$
8:         $wv' = rgh'(t) + Y'_{brg}(t)$
9:         $y_{vcl}(t) = ODE45(M_{vcl}, C_{vcl}, K_{vcl}, wv, wv')$
10:        $F_t = -K_{vcl}[2] * (y_{vcl}(t) - wv) - C_{vcl}[2] * (y'_{vcl}(t) - wv')$
11:        $R = -M_{vcl}g - F_t$
12:        $F = F_0$
13:        $F(t) = R$
14:        $Y_{brg} = Newmark\beta(M_{brg}, C_{brg}, K_{brg}, F)$
15:        $r_n = Y_{brg}(t)$
16:     $F_0 = F$
17: **Return** Y_{brg}, y_{vcl}

---

4. The interaction force from the vehicle to the bridge F_t upgrades the original loading matrix F_0 to produce F. At this location, the bridge is required to be analyzed again with the updated force matrix. Here, Newmark-β method is used for bridge dynamics analysis [Newmark et al., 1959].

5. If the difference between the updated bridge displacement and the one that was applied in Step 2 is higher than a predefined threshold, the process should be repeated from Step 2 onward by the updated bridge response. Otherwise, the vehicle moves to the next DOF on the bridge.

Step 5 in this process (i.e., the `while` loop in Algorithm 1) is expensive since it results in multiple full bridge analysis iterations within a time step. This is quite significant when the bridge is discretized with a large number of DOFs or is modeled with nonlinear elements. Figure 2 summarizes the approaches one can take for calculation of the sensing vehicle's measurement. In case (a), the brute-force approach is shown in which all the vehicles are coupled with the bridge.

1.3 Simplified Model

This study proposes a fast and accurate simulation approach for VBI problems in which: (1) the bridge span is medium to long and it is flexible, and (2) the vehicle network load is modeled as a random spatio-temporal load over the bridge span. The second condition refers to the ambient vibrations caused by a network of moving vehicles [De Roeck et al., 2000, Ren et al., 2004, Ren and Zong, 2004, Pakzad et al., 2008].

Figure 2b shows a simplified representation of Figure 1a, in which the traffic network (the sensing agent excluded) is replaced with an applied ambient white noise load while the sensing agent is still interacting with the bridge in a coupled fashion. While this approach is significantly computationally less expensive, the coupled system still requires iterations to reach the compatibility between the vehicle and the bridge at each time step. In this paper, we present an approach in which the compatibility calculations between two interacting components are not iterative, as shown in Figure 2c. In this approach, we posit that the dynamical effect of an individual sensing agent on a bridge response is negligible when the bridge is medium to long and the cumulative effect of other loads (the individual vehicle excluded) is significantly greater than a single vehicle. The approach is presented in Algorithm 2:

Algorithm 2 Simplified non-iterative VBI simulation.

1: **Input**: $M_{brg}, C_{brg}, K_{brg}, M_{vcl}, C_{vcl}, K_{vcl}, F_0, rgh$
2: $Y_{brg} = Newmark\beta(M_{brg}, C_{brg}, K_{brg}, F_0)$
3: **for** t = 1, $\cdots$, T **do**
4:     $r = Y_{brg}(t)$
5:     $wv = rgh(t) + r$
6:     $wv' = rgh'(t) + Y'_{brg}(t)$
7:     $y_{vcl}(t) = ODE45(M_{vcl}, C_{vcl}, K_{vcl}, wv, wv')$
8: **Return** Y_{brg}, y_{vcl}

In this algorithm, the bridge is only analyzed once at the beginning under $\boldsymbol{F}_0$. The bridge response is then linearly superimposed with rgh and then, applied to the vehicle dynamical model. In fact, the approach is similar to the constant force method proposed in González [2010]. However, in our approach the vehicle dynamics is incorporated in the vehicle response, which was not the case in a moving mass model. The approach has not been proposed or utilized previously; yet needs to be fully justified and evaluated. In the rest of this paper, we first propose a theoretical proof on a simplified case of the coupled VBI problem. This part intends to demonstrate that bridge to vehicle mass and stiffness ratios are the keys to determine the coupling degree. In the next step, VBI responses of multiple bridges with different characteristics and vehicles are numerically simulated using coupled (i.e., conventional) and uncoupled (i.e., simplified) procedures and results are compared. Discussions and comparison of the numerical results are also supplemented in the last sections.
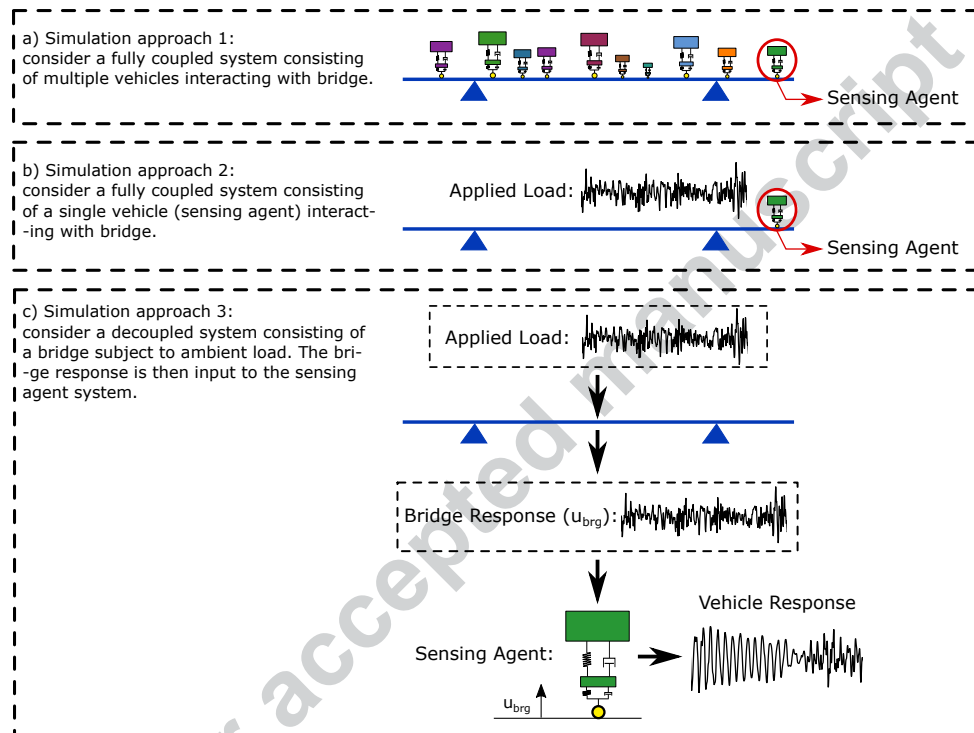

Figure 2: Simulation approaches: a) a complex and coupled system of a vehicle network interacting with a bridge; b) a coupled system of the sensing vehicle interacting with the bridge. The bridge is separately subject to an ambient load to capture the vehicle network's load; c) the proposed approach in which the bridge is only subject to the ambient load. The response is then applied to an uncoupled model of the sensing vehicle to produce the vehicle output.

2 Theoretical Approach

In this section, a closed-form theoretical proof for validity of the simplified model is presented. Generally, vehicle-bridge interaction is a complex model to be solved in closed-form, however, simplified models can be used for proof of concept [Frỳba, 2013, Yang et al., 2004a]. The objective here is to show that a coupled VBI system subject to external stochastic excitations produces bridge and vehicle responses that are very close to the responses of an uncoupled system, especially if the bridge is long and heavy. For this purpose, the mass and spring system shown in Figure 3 is considered in which the vehicle is located at the mid-span of the beam with no motion and in full interaction (no damping is considered for simplicity). The random spatio-temporal load of the bridge is also lumped into an effective point load that is applied to the bridge mass. In particular, the proof intends to show that the coupling of the bridge response x_b to the vehicle interaction decays as the bridge dimensions grow.

From Figure 3, the beam is modeled as a unidirectional spring, while the vehicle is a single DOF system. The bridge spring represents the first modal stiffness of the beam. The bridge mass is lumped at the contact point of the two components. The setup constitutes a 2 DOF coupled system with the equation of motion shown in Equation 1. Using this simplified setup, both responses are calculated in closed-form:
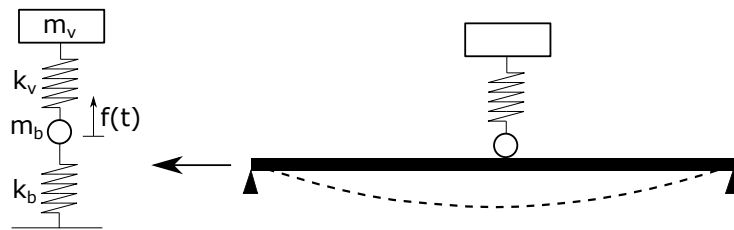
Figure 3: schematic of the coupled setup

$$\begin{bmatrix} m_b & 0 \\ 0 & m_v \end{bmatrix} \begin{bmatrix} \ddot{x}_b \\ \ddot{x}_v \end{bmatrix} + \begin{bmatrix} k_b + k_v & -k_v \\ -k_v & k_v \end{bmatrix} \begin{bmatrix} x_b \\ x_v \end{bmatrix} = \begin{bmatrix} f(t) \\ 0 \end{bmatrix} \tag{1}$$

where m_b and m_v are the bridge and vehicle masses, respectively; Also, k_b and k_v are the stiffnesses for two components. For further calculations, it is assumed that $m_b = \alpha m_v = \alpha m$ and $k_b = \beta k_v = \beta k$ in which α and β are bridge to vehicle mass and stiffness ratios, respectively, and $\alpha > \beta$. Therefore, using relative mass and stiffness ratios, Equation 1 can be states as:

$$\begin{bmatrix} \alpha m & 0 \\ 0 & m \end{bmatrix} \ddot{X} + \begin{bmatrix} (1+\beta)k & -k \\ -k & k \end{bmatrix} X = \begin{bmatrix} f(t) \\ 0 \end{bmatrix} \tag{2}$$

in which $X = [x_b; x_v]$ contains the bridge and vehicle responses, respectively. In order to solve this equation for X, the first step is to decouple it by using modal transformation using eigenvalue analysis shown in Equation 3.

$$det \begin{pmatrix} (\beta+1)k - \alpha m\omega^2 & -k \\ -k & k - m\omega^2 \end{pmatrix} = ((\beta+1)k - \alpha m\omega^2)(k - m\omega^2) - k^2 = 0 \tag{3}$$

By assuming $\frac{m\omega^2}{k} = \lambda$ and dividing both sides by k^2 we have:

$$(\beta+1) - (\beta+1)\lambda - \alpha\lambda + \alpha\lambda^2 - 1 = 0$$
$$\lambda = \frac{\alpha + \beta \pm \sqrt{(\alpha+\beta+1)^2 - 4\alpha\beta}}{2\alpha} \tag{4}$$

One can simply assume that $\alpha + \beta + 1 \approx \alpha + \beta$ since ratios are significantly large (especially the mass ratio α) when considering commercial vehicles and mid- to long-span bridges. This helps further simplifications as shown in Equation 5:

$$\lambda = \frac{\alpha + \beta \pm \sqrt{(\alpha+\beta)^2 - 4\alpha\beta}}{2\alpha} = \frac{\alpha + \beta \pm (\alpha - \beta)}{2\alpha}$$
$$\lambda_1 = 1 \Rightarrow \omega_1 = \sqrt{\frac{k}{m}} = \omega_v$$
$$\lambda_2 = \frac{\beta}{\alpha} \Rightarrow \omega_2 = \sqrt{\frac{\beta}{\alpha}}\omega_v \tag{5}$$

It is worth noting that from Equation 5, one of the natural frequencies is equal to the vehicle's fundamental frequency. Once the eigenvalues are found, eigenvectors can be derived to allow for modal superposition. For brevity, this calculation is summarized and the final mode shapes are presented in Equation 6.

$$\Phi = \begin{bmatrix} \frac{1}{\beta-\alpha+1} & \frac{\alpha-\beta}{\alpha} \\ 1 & 1 \end{bmatrix} = \begin{bmatrix} \phi_{11} & \phi_{12} \\ \phi_{21} & \phi_{22} \end{bmatrix} \tag{6}$$

In Equation 1, $f(t)$ is the applied load function, which is ultimately assumed as an ambient white noise for a random traffic network (i.e., Gaussian white noise $\sim \mathcal{N}(0, \sigma^2)$). In order to calculate the response of the system to such loads, one approach is to convert it to a sum of sinusoidal waves using Fourier transform. For a white noise, the spectral density function is a continuous function of a constant value (the value equals σ^2). Therefore, for simplicity, the response of the system subject to a single sinusoidal load is found in closed-form and then, the effect of different frequencies is evaluated by parametric study to determine whether the same conclusion is valid over the entire frequency band. Therefore, $f(t) = A_e sin(\omega_e t)$ is defined, in which A_e and ω_e are the sinusoidal amplitude and frequency, respectively. To convert the equation of motion shown in Equation 1 to modal coordinates, we premultiply both sides by Φ^T. The modal force vector and modal stiffness are then calculated as shown in Equation 7:

$$\Phi^T F(t) = \begin{bmatrix} \frac{1}{\beta-\alpha+1} & 1-\frac{\beta}{\alpha} \\ 1 & 1 \end{bmatrix}^T \begin{bmatrix} A_e sin(w_e t) \\ 0 \end{bmatrix} = \begin{bmatrix} \frac{A_e}{\beta-\alpha+1} sin(w_e t) \\ \frac{A_e(\alpha-\beta)}{\alpha} sin(w_e t) \end{bmatrix}$$

$$\hat{K} = \Phi^T K \Phi = \begin{bmatrix} \hat{k}_1 & 0 \\ 0 & \hat{k}_2 \end{bmatrix} = \begin{bmatrix} \left[\frac{\alpha}{(\beta-\alpha+1)^2} + \frac{\alpha-\beta-2}{\beta-\alpha+1} \right] k & 0 \\ 0 & \left[\frac{\beta^3+(1-2\alpha)\beta^2+\beta\alpha^2}{\alpha^2} \right] k \end{bmatrix}$$

$$x_b = \phi_{11}q_1 + \phi_{21}q_2$$

$$\hat{m}_1 \ddot{q}_1 + \hat{k}_1 q_1 = \frac{A_e}{\beta - \alpha + 1} sin(w_e t)$$

$$\hat{m}_2 \ddot{q}_2 + \hat{k}_2 q_2 = \frac{A_e(\alpha - \beta)}{\alpha} sin(w_e t) \tag{7}$$

The steady-state responses of the single-degree of freedom systems subject to a harmonic load have the following form shown in Equation 8:

$$q_1(t) = \frac{\frac{A_e}{\beta-\alpha+1}}{\hat{k}_1} \frac{1}{1-\gamma^2} . sin(\omega_e t)$$

$$q_2(t) = \frac{\frac{A_e(\alpha-\beta)}{\alpha}}{\hat{k}_2} \frac{1}{1-\frac{\alpha}{\beta}\gamma^2} . sin(\omega_e t) \tag{8}$$

in which $\gamma = \omega_e/\omega_v$. For a unit amplitude of the external load (i.e., $A_e = 1$) and by substitution of stiffness from Equation 7 to Equations 8, the harmonic amplitudes are calculated as follows:

$$amp(q_1) = \frac{\beta - \alpha + 1}{(\gamma^2 - 1)(\alpha^2 - 2\alpha\beta - 4\alpha + \beta^2 + 3\beta + 2)k}$$

$$amp(q_2) = \frac{\alpha(\alpha - \beta)}{(\beta - \alpha\gamma^2)(\alpha^2 - 2\alpha\beta + \beta^2 + \beta)k} \tag{9}$$

Finally, by modal superposition of two modal responses, the amplitude of the total harmonic vibration of the bridge is calculated as shown in Equation 10:

$$amp(x_b) = \phi_{11} \times amp(q_1) + \phi_{21} \times amp(q_2) =$$

$$\frac{1}{k} \left[\frac{1}{(\gamma^2 - 1)(\alpha^2 - 2\alpha\beta - 4\alpha + \beta^2 + 3\beta + 2)} + \frac{(\alpha - \beta)^2}{(\beta - \alpha\gamma^2)(\alpha^2 - 2\alpha\beta + \beta^2 + \beta)} \right] \tag{10}$$

So far, the bridge response from the fully coupled setup is derived. In order to find the bridge response using the second approach (i.e., the simplified model), the setup shown in Figure 4 is assumed. The bridge model is individually subject to the external load and responds to it. The response is then applied to an isolated vehicle model to produce the vehicle response. The closed-form solution for the bridge response in such an uncoupled setup is trivial and shown in Equation 11.
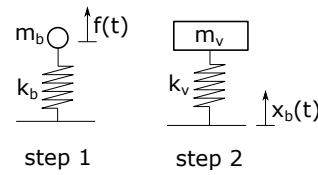
Figure 4: schematic of the uncoupled setup

$$m_b \ddot{x}_b + k_b x_b = A_e sin(\omega_e t)$$

$$x_b = \frac{A_e}{k_b} . \frac{1}{1 - \frac{\omega_e}{\omega_b}^2} . sin(\omega_e t)$$

$$amp(x_b) = \frac{1}{k(\beta + \alpha \gamma^2)} \tag{11}$$

Once Equations 10 and 11 are derived, the parametric study can take place. Both equations are functions of α, β, and γ. By plotting the response error between these two solutions for different ranges of these three parameters, the extent of the error in the simplified decoupled model can be investigated. Intuitively, as the bridge size increases, the stiffness of the structure decreases (i.e., longer bridges are more flexible), and the mass increases, resulting lower fundamental frequencies. The main objective is to observe the sensitivity of the error to the bridge size. Therefore, different mass and stiffness ratio pairs are plugged into both equations and errors are calculated. In addition, different loading frequencies are also examined. The mass and stiffness ratios (α and β) used for this purpose range $[50 : 10,000]$ and $[500 : 10]$, respectively, modeling short (stiff) bridges to long (flexible) ones. Loading frequencies spread exponentially from 10^{-3}Hz to 10^3Hz to envelope a sufficiently wide range of loading frequencies. Figure 5 summarizes the outcomes of the parametric study. Note that the x axis corresponds to different mass and stiffness ratio pairs, which is normalized to better convey the qualitative aspect of the plot (i.e., 0 is the stiffest bridge while 1 stands for the most flexible one).

Figure 5 demonstrates that based on the closed-form solutions, what would be the extent of error in the simplified simulation method for different types of bridges. As the bridge size increases, the error between two methods decays substantially (e.g., below 0.1% error for long bridges). This supports the idea that an uncoupled simplified solution is accurate enough when the bridge length increases. The figure also shows that there is a range of bridges in which the error is not negligible (for relatively short bridges the error can be up to 50% when the loading frequency resonate with the natural frequency of the vehicle). Also notice that the same trend occurs for different loading frequencies, with maximum error near the vehicle resonance frequency.

In this part, using our simplified model we showed that the uncoupled simulation approach yields accurate results when compared to the fully coupled approach, especially when the bridge size grows. In the next section, the results from a more detailed numerical simulation of the vehicle-bridge interaction are presented in order to incorporate other aspects of the VBI problems, such as vehicle motions and road roughness profile.

3   Numerical Analysis

In this section, the VBI problem is modeled numerically in Matlab and the results are compared with the signals from the simplified simulation approach. In this numerical case study, six bridges with different span lengths are modeled in SAP2000 and two simulation approaches are implemented. The exact numerical approach for modeling the bridge response interacting with a moving vehicle (roughness included) is adopted from González et al. [2012] as presented in Algorithm 1.

The bridge setup is shown in Figure 6. The span varies from 15 m (very short and stiff bridge) to 500 m (long and flexible bridge), with mechanical properties shown in Table 1. The bridge is 3D modeled in SAP2000 using prismatic beams with box cross-sections. Note that the considered single span simply-supported bridge is the use case for the majority of numerical studies in the VBI community [Yang et al., 2004b, OBrien et al., 2010]. Since one of the objectives of our paper is to propose a simplified numerical approach for VBI analysis, the same geometry and boundary condition are considered in the first numerical case study. The reason for a 3D model of the bridge is to have a physical sense of the dimensions of the deck section and better visualization. The modeling process is as follows: The bridge geometry and material are defined in the SAP model. The stiffness and mass matrices of the SAP model are then exported to a MATLAB script within which bridge dynamic analyses as well as vehicle-bridge interactions
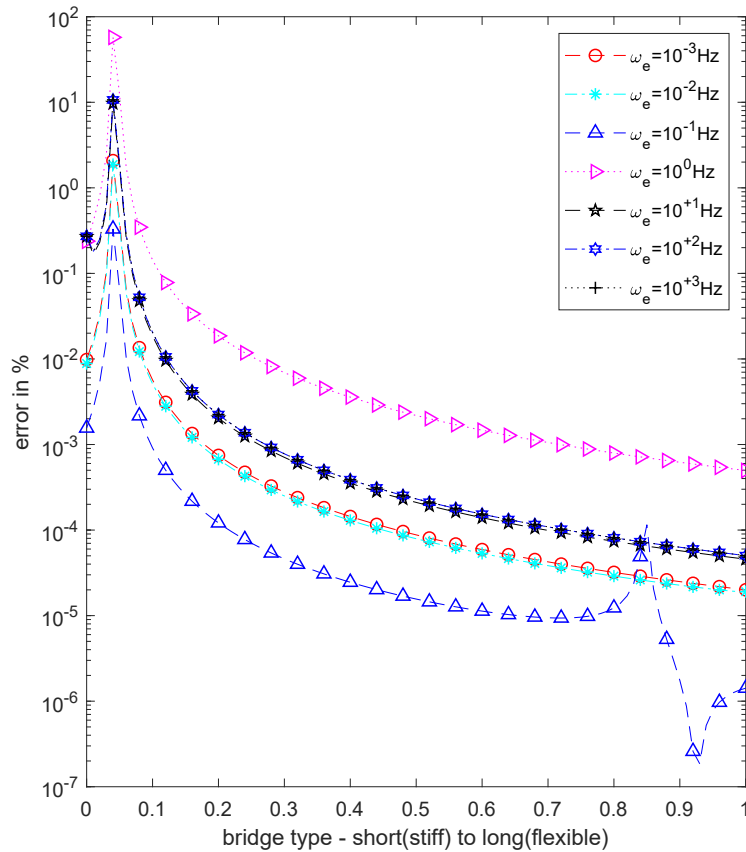
Figure 5: Results of the theoretical approach: parametric study shows the extent of the error for different bridge types and loading frequencies when using the simplified bridge-vehicle simulation approach.
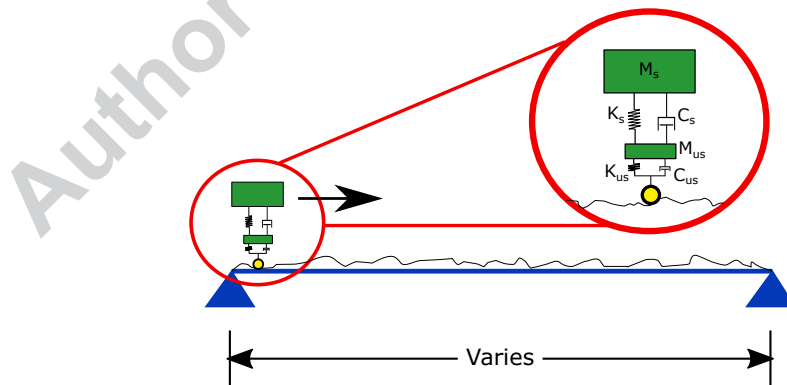

Figure 6: Schematic of simulated model - roughness profile is also included

are held. The accuracy of the bridge models is verified by examining bridge natural frequencies. The fundamental modes in shorter bridges are vertical (longitudinal) while for very long spans, torsional modes dominate. Note that the torsional modes are not within the scope of this study and are excluded from modal analyses. In this case study, bridges are all simply-supported; however, a different geometry is evaluated in Section 5. The structural behavior is assumed linear elastic for consistency with operational modal analysis. The study does not take large deformations

9

and nonlinearities into account based on the fact that the method is being proposed for numerical simulation of bridges under operational mode. In particular, no material nonlinearity is expected here. In terms of geometry nonlinearity, we expect that it may be effective for very long bridges.

In this study, bridge models are deterministic and no uncertainty for material and geometry is included. In fact, the study is focused on studying the extent of bridge-vehicle interaction with respect to bridge dimensions and traffic level. Ni et al. [2019] showed that by incorporating uncertainties in bridge modeling, the modal properties are changed, however, this variation is dramatically lower for the fundamental modes compared to higher ones. In addition, Yang and Lin [2005] showed that in a vehicle-bridge interaction scenario, the bridge response is highly dominated by the first natural mode. Considering these, uncertainty propagation analysis is neglected in this study. The road roughness profile is adapted according to ISO standard for a road class 'A' [de Normalización , Ginebra] which is the case for a well maintained highway road condition. At each time instance, the bridge model is analyzed dynamically using Newmark-β method using matrices imported from SAP2000. For the vehicle, first a quarter-car model is adopted with the properties shown in Table 2. This vehicle simulates suspension properties of a commercial vehicle with high damping and low natural frequency (which are critical factors for a comfortable ride [Milliken et al., 2002]). The second vehicle is a quarter-car model of a heavy truck adopted from [Harris et al., 2007, Elhattab et al., 2016] with properties shown in Table 3. The second vehicle is selected to investigate the approximation error of using the simplified method for heavy sensing agents when the weight is not negligible.

Table 1: Bridge spans and cross-section dimensions

Span length [m]	*15m*	*30m*	*50m*	*100m*	*200m*	*500m*
Outside depth [m]	0.60	1.10	1.60	2.40	3.00	5.00
Outside width [m]	0.3	0.50	1.30	2.00	2.50	4.00
Flange thickness [m]	0.04	0.05	0.10	0.15	0.15	0.50
Web thickness [m]	0.02	0.03	0.05	0.10	0.10	0.25
Fundamental freq. [Hz]	8.03	3.63	2.05	0.75	0.24	0.06

Table 2: Commercial vehicle properties

Property Name	*Value*	*Units*
Unsprung Mass	69.9	Kg
Sprung Mass	466.0	Kg
Tire Damping	0.0	Ns/m
Suspension Damping	2796.0	Ns/m
Tire Stiffness	3043.0	N/m
Suspension Stiffness	290.3	N/m
Fundamental Frequency	1.2	Hz

Table 3: Heavy truck properties

Property Name	*Value*	*Units*
Unsprung Mass	700.0	Kg
Sprung Mass	17,300.0	Kg
Tire Damping	0.0	Ns/m
Suspension Damping	1.0×10^4	Ns/m
Tire Stiffness	1.75×10^6	N/m
Suspension Stiffness	4.0×10^5	N/m
Fundamental Frequency	0.69	Hz

For a fair comparison, the vehicle's speed is kept constant among all bridge spans ($10m/sec$). Finally, the traffic load is modeled as a random ambient load uniformly applied over the span with the amplitude proportional to the number of vehicles. In particular, for n vehicles, a random and sparse matrix is generated in which the sum of forces in each row (i.e., for each time instance) is equal to $n \times 2,000 \times g$ N, assuming $2,000$ kg for the average weight of a commercial vehicle and g is the gravity acceleration. Four traffic levels are considered for each span length with $n = 0, 10, 20, 50$ ($n = 0$ models an isolated bridge while $n = 50$ models a bridge with 50 vehicles moving while being scanned by the sensing agent). The bridge is modeled as a MDF system with $0.1m$ spatial discretization (e.g., 15 m long bridge is modeled with 150 DOFs). The $0.1m$ discretization is selected based on a trade-off between computation time and maximum avoidance for displacement interpolation when the vehicle's location falls inside a bridge segment. 0.1m-long bridge segmentation yields exact vehicle displacement calculation when vehicles' speed is set to 10m/sec. For vehicles moving faster than this speed, discretization of vehicle's time and space coordinates causes some gaps in locations of consecutive time steps. This gap causes a simplification in the vehicle's initial condition (particularly the initial speed) calculation. However, in this study the damping of the unsprung mass is set to zero which disconnects the vehicle's dynamic analysis to its initial speed. For simulating responses using the decoupled model, Algorithm 2 is adopted: the random traffic load is firstly applied to the bridge with no consideration for the sensing vehicle. The bridge responses at the vehicle locations are then aligned in space and applied to the model of the sensing vehicle. The vehicle processes the input through its dynamical model (shown in Tables 2 and 3) and produce the vehicle response.
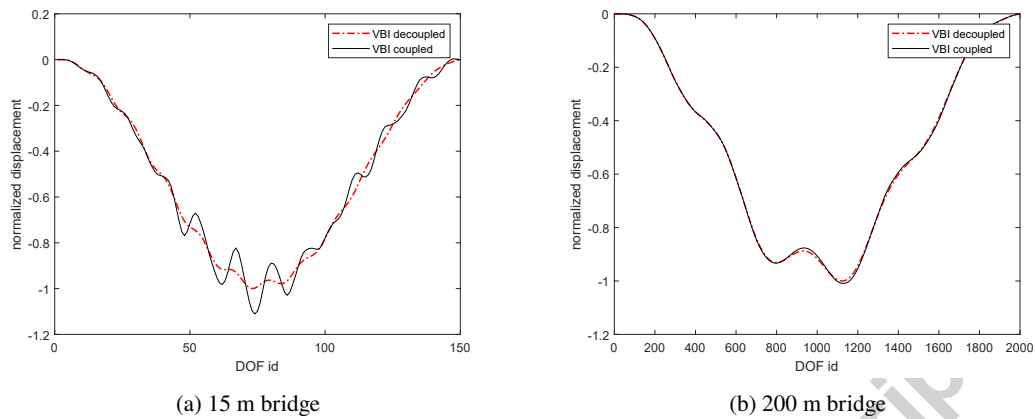
(a) 15 m bridge

(b) 200 m bridge

Figure 7: Bridge displacement simulation results for the commercial vehicle
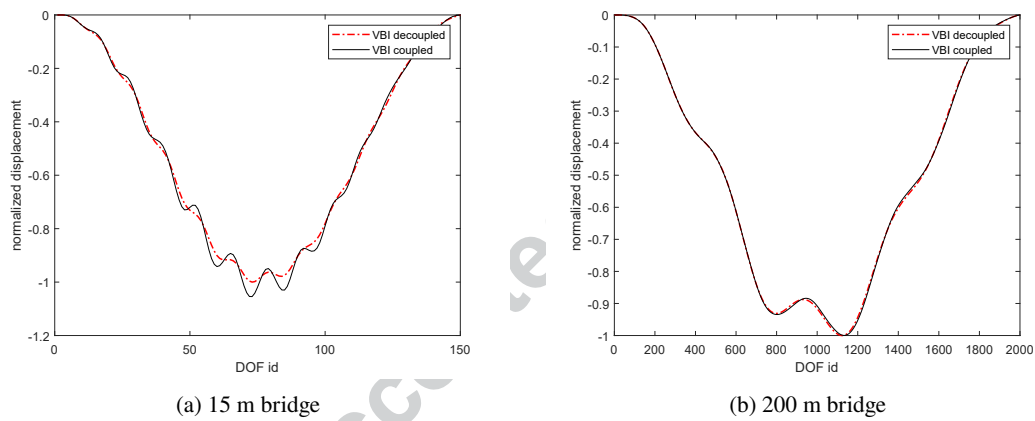

(a) 15 m bridge

(b) 200 m bridge

Figure 8: Bridge displacement simulation results for the heavy truck

The performance of the simplified model is evaluated in terms of the bridge response as well as the vehicle response. From Section 2 it is expected that the simplified model yield more accurate response estimations as the length of the bridge span increases. For the conventional simulation approach, the acceptance threshold for the bridge response is set to 1.5×10^{-12} m. For each bridge span and traffic level pairs, bridge and vehicle response signals are simulated using two approaches (in total 24 runs for each vehicle); and the errors between two signals are measured in time and frequency domains using the mean squared error (MSE). For more consistency, the responses are scaled by the absolute maximum values of the displacement signals found from the conventional method.

Simulated displacement signals for two spans (15 m and 200 m) are shown in Figures 7 and 8. For both vehicle types, the bridge response differs noticeably between the conventional and simplified VBI simulations for the 15 m bridge. However, as expected from Section 2, as the bridge length increases, the discrepancy between two simulation approaches shrinks in bridge response estimation. The MSE values versus bridge length are also presented in Figures 9 and 10 for the commercial vehicle and Figures 11 and 12 for the heavy truck to further quantify this observation. Figures 9 and 11 (error in the bridge response simulations) show a strictly decreasing MSE value as the bridge length increases. In addition, in both cases, as the traffic level increases (i.e., from $n = 0$ to $n = 50$), the estimation error reduces. This is more evident for the commercial vehicle. Note that the same patterns are deduced from the frequency representation plots.

Figures 9 and 11 show the extent of error for simulating stationary sensors' data that are attached to the bridge. However, what a mobile sensing agent records while scanning the bridge, is not the bridge pure vibrations, but the vehicle response to it. Therefore, Figures 10 and 12 show the accuracy of the vehicle response subject to the bridge motion when comparing the simplified model with the conventional approach. In this case, two sensing agents (i.e., the commercial vehicle versus the heavy truck) react differently. For the commercial vehicle, the responses are relatively

11

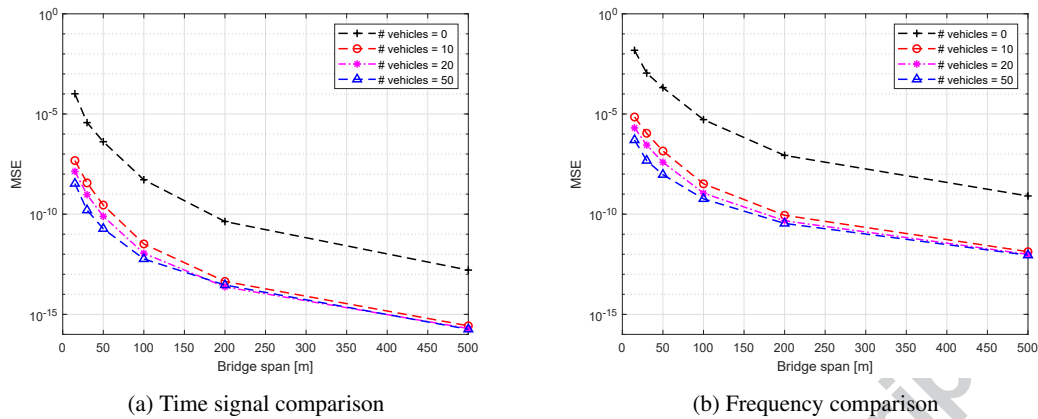(a) Time signal comparison (b) Frequency comparison

Figure 9: Bridge response comparison for the commercial vehicle in terms of the MSE: The trends show more accurate simulation results as bridge span or traffic volume increases.
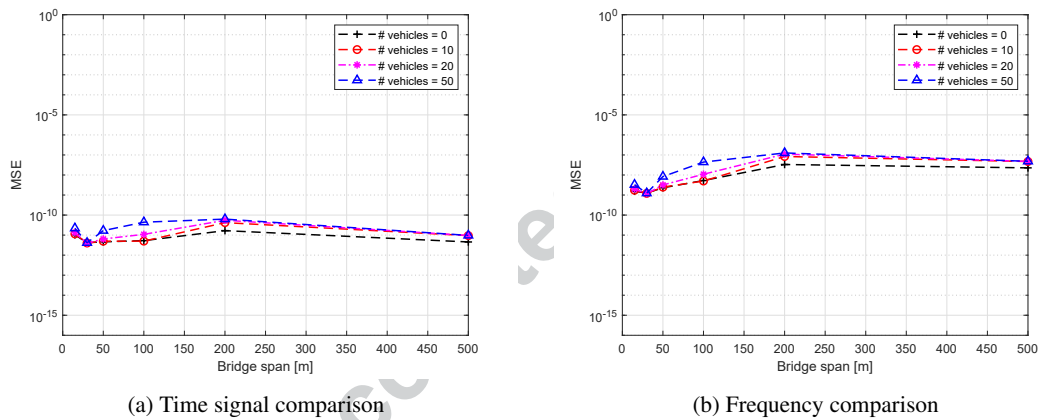

(a) Time signal comparison (b) Frequency comparison

Figure 10: Vehicle response comparison for the commercial vehicle in terms of the MSE: The trends show invariance to the span and the traffic level.

insensitive to the span and traffic level and the errors are consistently low for all cases. However, from Figure 12, the truck response is simulated less accurately when the bridge span grows from 15 m to 100 m (for longer bridges, a decaying error trend is observed again). In particular, the frequency estimation error for the heavy vehicle crossing a 100 m long bridge is quite noticeable when using the simplified model. From Table 3, the fundamental frequency of the truck is 0.69Hz which is near resonance for the 100 m long bridge (from Table 1, $f = 0.75$Hz). Moreover, the vehicle weight is significant, which results in higher interaction forces applied to the bridge and the vehicle itself. In fact, this case highlights that when the bridge and the vehicle have near resonance frequencies, the simplified model works more accurately when the vehicle is lightweight. To validate this, the properties from Table 3 are downscaled by a factor of 5 (i.e., the same natural frequency while being lighter) and simulation for 100 m long bridge is repeated. The MSE value for $n = 50$ from 1.19×10^{-4} reduced to 5.46×10^{-6}.

4 Computational Cost Evaluation

The main objective of the simplified model is to improve the computational performance of simulations while having a minimal impact on the accuracy of the results. In Figure 13 the computational runtimes for the commercial vehicle simulation case are compared between two methods (the heavy vehicle yields a very similar plot as well). The figure elaborates that while the runtime increases linearly in the simplified model, it grows exponentially when using the conventional approach for longer bridges. For instance, using a single Intel Core i5 CPU, the entire VBI simulation process for the 500 m long bridge takes 1.8 sec using the simplified model, while the same process takes nearly 2,250.0

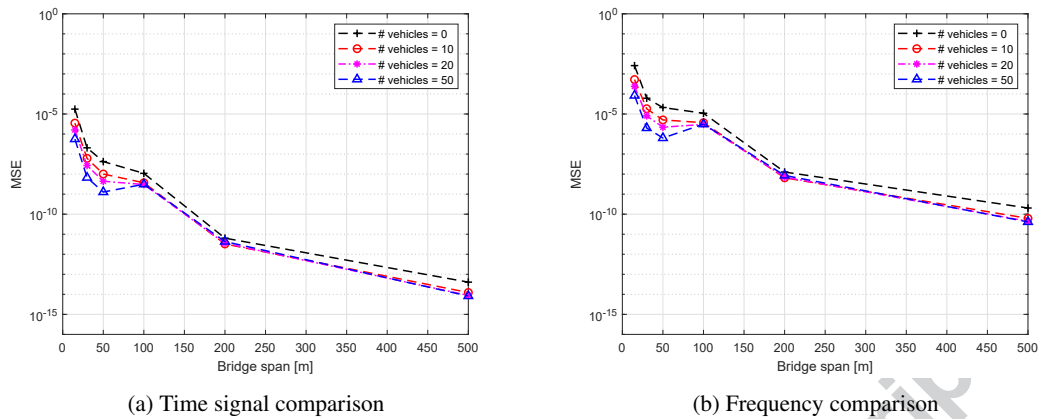(a) Time signal comparison

(b) Frequency comparison

Figure 11: Bridge response comparison for the heavy truck in terms of the MSE: The trends show more accurate simulation results as the bridge span or the traffic volume increases.

(a) Time signal comparison
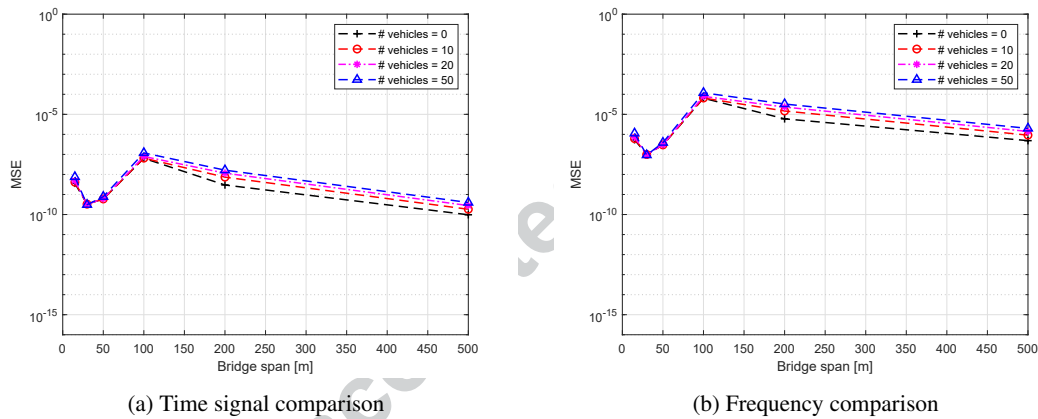
(b) Frequency comparison

Figure 12: Vehicle response comparison for the heavy truck in terms of the MSE: The trends show that the error peaks when the bridge and the vehicle have close fundamental frequency values.

sec using the conventional method (more than $1,000x$ slower). This dramatic runtime difference is resulted by the inner iterations of the conventional approach (see Algorithm 1) that guarantee the compatibility. Within this iteration, the entire bridge model has to be analyzed repeatedly for the modified interaction force as long as the stopping criterion is not met, which is computationally very expensive. This is a bottleneck for the numerical computation, especially when the bridge length increases or models with higher fidelity is of interest (i.e., MDF model grows in size). Alternatively, the simplified model fully decouples the bridge model from the vehicle systems, which yields a one-time bridge analysis (see Algorithm 2). This significant speedup enables to perform VBI simulations for medium- to long-span bridges with fine spatial discretization, which is required for numerical studies on crowdsensing-based health monitoring.

5   Fully Coupled Vehicle Network Simulation

In this section, a fully coupled network of vehicles is analyzed to verify the followings: (1) the premise of ambient white noise on behalf of a random traffic load is valid and (2) the simplified method yields accurate results for bridges with different geometries. Regarding that, a continuous bridge with four 50m-long spans with elastic steel material is modeled and shown in Figure 14 (beam cross-section is shown as well). The bridge length is discretized with 0.1m grids, resulting a 2,001 DOF system. The roughness profile is introduced with the same setup as before. In this case, instead of applying a spatio-temporal random load to model random traffic loads, the bridge is subjected to different levels of traffic caused by deterministic vehicle trajectories (as shown in Figure 2a). All vehicles are interacting with
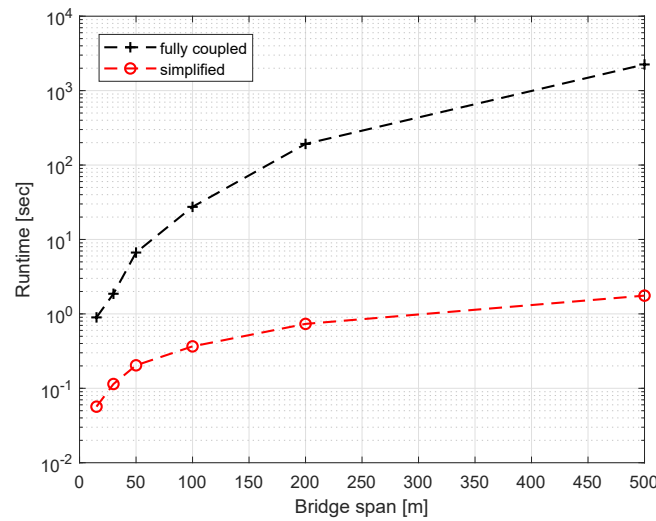
13

Figure 13: Runtime comparison between the conventional and simplified models: the conventional approach is computationally >1,000x slower than the simplified model for the 500 m bridge with no significant gain in the accuracy of response estimations.

the bridge in the same fashion as given in Algorithm 1. In summary, the convergence loop continues until all vehicles have reached acceptable displacement errors.
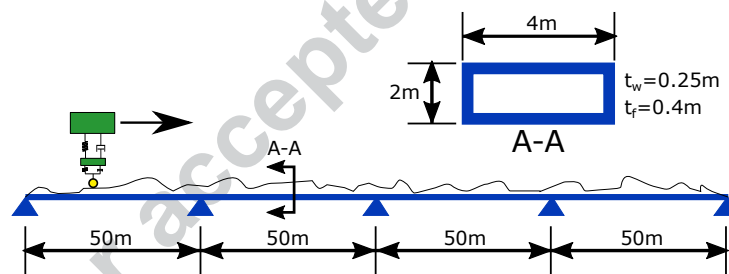

Figure 14: Geometry of four-span continuous bridge and cross-section.

In these analyses, each vehicle in the network has certain speed and mechanical properties. The mechanical properties are randomly selected with a lognormal distribution. The mean values for each property is set to the values given in Table 2 for the commercial vehicle. Standard deviation σ is also set to 0.35 for all components of the property table. The map of vehicle network trajectories for two levels of traffic is shown in Figure 15. In this figure, each column contains momentary response of the bridge at all DOFs. Each trajectory is represented by a line in the spatio-temporal response matrix. Different slopes show different directions and speeds (close to horizontal shows very low speed vehicles while nearly vertical ones show very fast bridge crossings). The random trajectory generator allows for fixed vehicles as well.

The first objective is to show the spatio-temporal load determined by the vehicle network and bridge interaction has statistical characteristics of a 2D white noise. The resulted loading matrix for a random traffic case (with 200 random vehicle trajectories) is derived from the coupled dynamic analysis and the Fourier transform is shown in Figure 16 along with the same representation of a white noise loading matrix. By comparison, both plots show uniform content everywhere with no coherent frequency peaks. This implies that a realistic loading scenario with deterministic vehicle motions has the similar effect to a random white noise.

In the next step, a mobile sensing agent is added to the traffic networks and the bridge interaction is considered with (1) conventional (Algorithm 1) and (2) simplified (Algorithm 2) approaches and results are compared. Three different speeds for the sensing agent are considered: $10m/sec$, $20m/sec$, and $30m/sec$. The MSE error between vehicle and bridge response estimations of the simplified and conventional approach is calculated and plotted in Figure 17. In
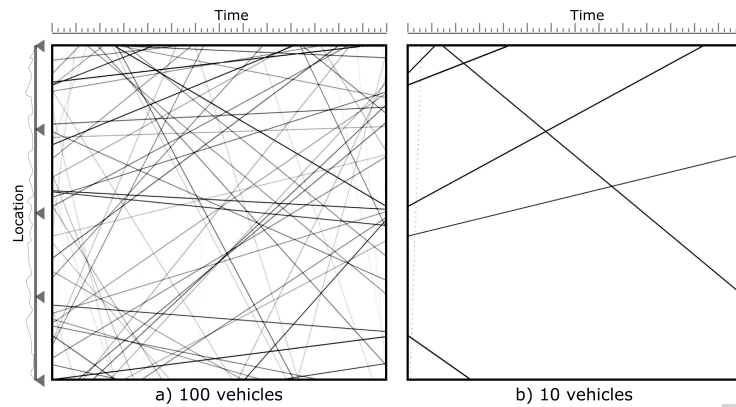
14

Figure 15: Random vehicles trajectory in the time-space matrix. Each solid line represents a single vehicle's motion over the bridge. Vehicles have different speeds and directions and all are fully interacting with the bridge. Two levels of traffic are shown.
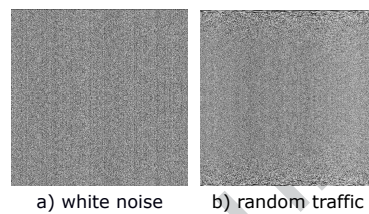

Figure 16: Frequency representation of spatio-temporal load applied to the bridge. (a) white noise spatio-temporal load considered in analyses in Section 3. (b) actual load resulted from a traffic network of random vehicles with full consideration for the vehicle-bridge interaction. Similarity between two representations confirm the random nature of traffic load.

all three speed cases, the error significantly drops when the network includes higher number of vehicles. This figure confirms that even in a realistic simulation of the traffic network, the simplified approach yields accurate estimations for the majority of cases (i.e., when the network is sufficiently crowded). As for the sensing agent's speed effect, except for a slightly higher errors for higher speeds, other variations are not conclusive. By comparing these plots with Figures 9 and 10, the trends are consistent. The variations in the magnitude of the MSEs can be explained due to different bridge boundary conditions and more realistic loading pattern.
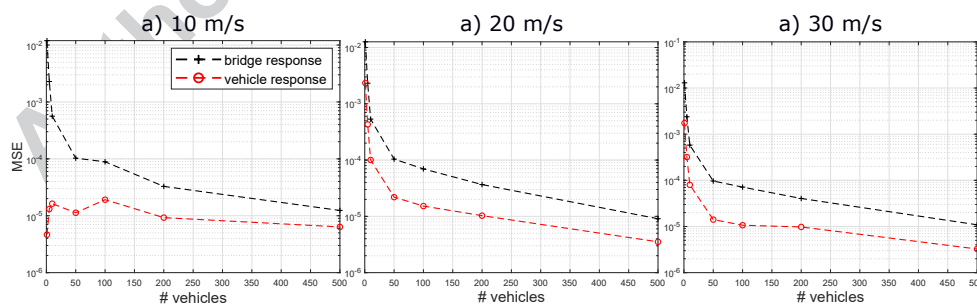

Figure 17: Bridge and vehicle response comparison for a commercial sensing vehicle in terms of the MSE: the plots confirm that as the number of traffic fleet increases, the error in simplified approach reduces. In general, once the number of fleet tops 50, the accuracy of the proposed method is very high.

6   Conclusions

In this paper, a modified simulation algorithm was proposed for vehicle-bridge interaction (VBI) problems concerning medium- to long-span bridges with random traffic excitation. The primary deliverable of this study to the SHM

15

community is to enable a fast and accurate numerical analysis method that can be used in different bridge infrastructure management levels, such as (1) evaluation of crowdsensing-based methods for bridge modal identification and (2) probabilistic and life-cycle analysis of bridges subjected to vehicle networks under various uncertainties (e.g., road profile, vehicle dynamics, traffic level, and environmental variations). Our main contribution is the result that as the bridge flexibility increases (longer spans), the degree of coupling between the vehicle and the bridge reduces notably. Conventional VBI simulation algorithms require iterations within each time step in order to reach a desired level of compatibility between the vehicle and the bridge, which is computationally expensive. We show that the proposed simple, decoupled model is efficient for simulations of the vehicle-bridge interacting systems in such cases, with an accuracy that increases with bridge flexibility. In particular, the theoretical analysis showed that the response of a coupled continuous beam and vehicle setup subject to a random load becomes more independent to the vehicle dynamics as the bridge mass grows and the stiffness reduces. Therefore, for longer or flexible bridges, the dynamics are practically independent. Moreover, the numerical simulation validated that the bridge size and traffic load intensity both affect the accuracy of the bridge vibration estimations using the simplified model. For commercial vehicles, the simplified method yields accurate response estimations. In the case of a heavy vehicle with a natural frequency near the bridge's fundamental frequency, e.g., heavy vehicles and flexible bridges, the error associated with the simplified model is noticeable. In terms of the computational cost, a comparative study showed that the cost of the conventional model behaves exponentially while the cost of the simplified model is linear.

7 Acknowledgments

References

SR Chen and CS Cai. Equivalent wheel load approach for slender cable-stayed bridge fatigue assessment under traffic and wind: Feasibility study. *Journal of Bridge Engineering*, 12(6):755–764, 2007.

XQ Zhu and Siu-Seong Law. Structural health monitoring based on vehicle-bridge interaction: accomplishments and challenges. *Advances in Structural Engineering*, 18(12):1999–2015, 2015.

XQ Zhu and Siu-Seong Law. Recent developments in inverse problems of vehicle–bridge interaction dynamics. *Journal of Civil Structural Health Monitoring*, 6(1):107–128, 2016.

YB Yang and Judy P Yang. State-of-the-art review on modal identification and damage detection of bridges by moving test vehicles. *International Journal of Structural Stability and Dynamics*, 18(02):1850025, 2018.

Soheil Sadeghi Eshkevari, Thomas J. Matarazzo, and Shamim N. Pakzad. Bridge modal identification using acceleration measurements within moving vehicles. *Mechanical Systems and Signal Processing*, 141:106733, 2020a. ISSN 0888-3270. doi: https://doi.org/10.1016/j.ymssp.2020.106733.

Yufen Zhou and Suren Chen. Vehicle ride comfort analysis with whole-body vibration on long-span bridges subjected to crosswind. *Journal of Wind Engineering and Industrial Aerodynamics*, 155:126–140, 2016.

A Camara, I Kavrakov, K Nguyen, and G Morgenthal. Complete framework of wind-vehicle-bridge interaction with random road surfaces. *Journal of Sound and Vibration*, 2019.

Yeong-Bin Yang, JD Yau, Zhongda Yao, and YS Wu. *Vehicle-bridge interaction dynamics: with applications to high-speed railways*. World Scientific, 2004a.

Abdollah Malekjafarian and Eugene J OBrien. Identification of bridge mode shapes using short time frequency domain decomposition of the responses measured in a passing vehicle. *Engineering Structures*, 81:386–397, 2014.

Soheil Sadeghi Eshkevari, Shamim N Pakzad, Martin Takáč, and Thomas J Matarazzo. Modal identification of bridges using mobile sensors with sparse vibration data. *Journal of Engineering Mechanics*, 142(4):04015109, 2020b. doi: 10.1061/(ASCE)EM.1943-7889.0001733.

Kevin P O'Keeffe, Amin Anjomshoaa, Steven H Strogatz, Paolo Santi, and Carlo Ratti. Quantifying the sensing power of vehicle fleets. *Proceedings of the National Academy of Sciences*, 116(26):12752–12757, 2019.

Thomas J Matarazzo, Paolo Santi, Shamim N Pakzad, Kristopher Carter, Carlo Ratti, Babak Moaveni, Chris Osgood, and Nigel Jacob. Crowdsensing framework for monitoring bridge vibrations using moving smartphones. *Proceedings of the IEEE*, 106(4):577–593, 2018.

Francesco Calabrese, Massimo Colonna, Piero Lovisolo, Dario Parata, and Carlo Ratti. Real-time urban monitoring using cell phones: A case study in rome. *IEEE Transactions on Intelligent Transportation Systems*, 12(1):141–151, 2010.

Pu Wang, Timothy Hunter, Alexandre M Bayen, Katja Schechtner, and Marta C González. Understanding road usage patterns in urban areas. *Scientific reports*, 2:1001, 2012.

Yan Yu, Ruicong Han, Xuefeng Zhao, Xingquan Mao, Weitong Hu, Dong Jiao, Mingchu Li, and Jinping Ou. Initial validation of mobile-structural health monitoring method using smartphones. *International Journal of Distributed Sensor Networks*, 11(2):274391, 2015.

Maria Feng, Yoshio Fukuda, Masato Mizuta, and Ekin Ozer. Citizen sensors for shm: Use of accelerometer data from smartphones. *Sensors*, 15(2):2980–2998, 2015.

Ekin Ozer, Maria Feng, and Dongming Feng. Citizen sensors for shm: Towards a crowdsourcing platform. *Sensors*, 15(6):14591–14614, 2015.

Thomas J Matarazzo and Shamim N Pakzad. Stride for structural identification using expectation maximization: iterative output-only method for modal identification. *Journal of Engineering Mechanics*, 142(4):04015109, 2016.

Thomas J Matarazzo and Shamim N Pakzad. Scalable structural modal identification using dynamic sensor network data with stridex. *Computer-Aided Civil and Infrastructure Engineering*, 33(1):4–20, 2018.

Soheil Sadeghi Eshkevari and Shamim N Pakzad. Signal reconstruction from mobile sensors network using matrix completion approach. In *Topics in Modal Analysis & Testing, Volume 8*, pages 61–75. Springer, 2020.

Arturo González. Vehicle-bridge dynamic interaction using finite element modelling. In *Finite element analysis*. IntechOpen, 2010.

Ladislav Frỳba. *Vibration of solids and structures under moving loads*, volume 1. Springer Science & Business Media, 2013.

CW Lin and YB Yang. Use of a passing vehicle to scan the fundamental bridge frequencies: An experimental verification. *Engineering Structures*, 27(13):1865–1878, 2005.

Chul-Woo Kim and Mitsuo Kawatani. Pseudo-static approach for damage identification of bridges based on coupling vibration with a moving vehicle. *Structure and infrastructure engineering*, 4(5):371–379, 2008.

Eugene J OBrien, Daniel Cantero, Bernard Enright, and Arturo González. Characteristic dynamic increment for extreme traffic loading events on short and medium span highway bridges. *Engineering Structures*, 32(12):3827–3835, 2010.

Arturo González, Eugene J OBrien, and PJ McGetrick. Identification of damping in a bridge using a moving instrumented vehicle. *Journal of Sound and Vibration*, 331(18):4115–4131, 2012.

LRFD AASHTO. Bridge design specifications (2007). *American Association of State Highway and Transportation Officials, Washington, DC*, 4, 2008.

Nathan Mortimore Newmark et al. A method of computation for structural dynamics. American Society of Civil Engineers, 1959.

Guido De Roeck, Bart Peeters, and Wei-Xin Ren. Benchmark study on system identification through ambient vibration measurements. In *Proceedings of IMAC-XVIII, the 18th International Modal Analysis Conference, San Antonio, Texas*, pages 1106–1112, 2000.

Wei-Xin Ren, Issam E Harik, George E Blandford, M Lenett, Baseheart, and TM. Roebling suspension bridge. ii: Ambient testing and live-load response. *Journal of Bridge Engineering*, 9(2):119–126, 2004.

Wei-Xin Ren and Zhou-Hong Zong. Output-only modal parameter identification of civil engineering structures. *Structural Engineering and Mechanics*, 17(3-4):429–444, 2004.

Shamim N Pakzad, Gregory L Fenves, Sukun Kim, and David E Culler. Design and implementation of scalable wireless sensor network for structural monitoring. *Journal of infrastructure systems*, 14(1):89–101, 2008.

Y-B Yang, CW Lin, and JD Yau. Extracting bridge frequencies from the dynamic response of a passing vehicle. *Journal of Sound and Vibration*, 272(3-5):471–493, 2004b.

Pinghe Ni, Yong Xia, Jun Li, and Hong Hao. Using polynomial chaos expansion for uncertainty and sensitivity analysis of bridge structures. *Mechanical Systems and Signal Processing*, 119:293–311, 2019.

YB Yang and CW Lin. Vehicle–bridge interaction dynamics and potential applications. *Journal of sound and vibration*, 284(1-2):205–226, 2005.

Organización Internacional de Normalización (Ginebra). *Mechanical vibration-road surface profiles-reporting of measured data*. ISO, 1995.

William F Milliken, Douglas L Milliken, and Maurice Olley. *Chassis design: principles and analysis*, volume 400. Society of Automotive Engineers Warrendale, 2002.

Niall K Harris, Eugene J OBrien, and Arturo González. Reduction of bridge dynamic amplification through adjustment of vehicle suspension damping. *Journal of Sound and Vibration*, 302(3):471–485, 2007.

Ahmed Elhattab, Nasim Uddin, and Eugene OBrien. Drive-by bridge damage monitoring using bridge displacement profile difference. *Journal of Civil Structural Health Monitoring*, 6(5):839–850, 2016.